Food Chemistry: X 23 (2024) 101613

Contents lists available at ScienceDirect

Food Chemistry: X

journal homepage: www.sciencedirect.com/journal/food-chemistry-x

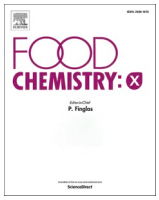

Structural characterization and mast cell stabilizing activity of Red-edge tea polysaccharide

Yan Li [a], Jinhao Pang [a], Yongfeng Lin [a], Wenmei Liu [b,c], Zehua Zou [b,c], Guangming Liu [a,*], Qingmei Liu [a,*]

[a] College of Ocean Food and Biological Engineering, Xiamen Key Laboratory of Marine Functional Food, Fujian Provincial Engineering Technology Research Center of Marine Functional Food, Jimei University, Xiamen 361021, Fujian, China
[b] San Ming MING BAWEI Industry Research Institute, Sanming 353000, China
[c] Changting County Green Economy Ecological Health Industry Research Institute, Longyan 366300, China

ARTICLE INFO

Keywords:
Anti-allergic activity
Mast cell stabilizing
Tea polysaccharide

ABSTRACT

The potential anti-allergic properties of tea have been demonstrated in studies supporting theanine and catechin. However, research on tea polysaccharides' anti-allergic properties has been limited. In this study, we extracted red-edge tea crude polysaccharide (RETPS) and evaluated its anti-allergic activity using the mast cell, passive cutaneous anaphylaxis, and passive systemic anaphylaxis models. We purified RETPS using the DEAE-52 cellulose column, analyzed its composition and structural characteristics, and compared the anti-allergic properties of different polysaccharide fractions. The purified components RETPS-3 and RETPS-4 displayed higher galacturonic acid content and lower molecular weight (106.61 kDa and 53.95 kDa, respectively) compared to RETPS (310.54 kDa). In addition, RETPS-3 and RETPS-4 demonstrated superior anti-allergic activity than RETPS in mice's passive cutaneous and systemic allergic reactions. Our findings provide evidence of the anti-allergic potential of tea polysaccharides and offer a theoretical foundation for developing tea polysaccharides as a functional anti-allergic food product.

1. Introduction

Food allergy (FA) is an immune disorder that manifests rapidly after consuming specific and poses a serious threat to the health of individuals with allergies (Sathe, Liu, & Zaffran, 2016). FA is a severe global health issue and its prevalence has been steadily increasing in recent decades (Saarimäki et al., 2023). Despite the growing number of affected individuals, medical treatment options for FA are limited due to the risks and costs associated with immunotherapy and the potential side effects of antiallergic drugs (Berin, 2023). Consequently, researchers are actively seeking natural bioactive substances with high efficacy and minimal side effects to alleviate food allergies. At present, oligosaccharides, polysaccharides, polyphenols, and other natural active substances have demonstrated anti-food allergy activities (Zhang et al., 2022). Among these, polysaccharides have garnered significant attention due to their ability to stabilize mast cells (Zhang et al., 2023), and repair damaged intestinal barriers (Liu et al., 2020).

Mast cells are considered both effector cells and immune regulatory cells that play an important role in FA. Hypersensitivity reactions, which are acute, systemic, and potentially life-threatening, are triggered by the degranulation of mast cells and basophils (Simons, 2008). These reactions occur when allergen-specific IgE antibodies bind to the high-affinity IgE receptor FcεRI on the surface of mast cells, leading to their activation and subsequent release of histamine and protease mediators (Oettgen, 2023). The rat basophilic leukemia (RBL-2H3) cell line is commonly employed to investigate the inhibitory activity of natural bioactive substances on mast cell activation due to its ability to express a range of mast cell characteristics and functions (Oettgen, 2023). *In vivo* evaluation of drugs with anti-allergic properties often employs the traditional models of IgE/mast cell-driven anaphylaxis in mice, known as passive cutaneous anaphylaxis (PCA) and passive systemic anaphylaxis (PSA), to provide initial assessments (Bryce et al., 2016; Nakajima et al., 2020).

Tea, with its distinct flavor and aroma, is the second most popular beverage worldwide, following water, owing to its nutritional value and numerous health benefits (Zhang et al., 2024). Various biologically active compounds, including alkaloids, tea polyphenols, tea polysaccharides (TPS), and tea pigments, contribute to tea's diverse

* Corresponding authors.
E-mail addresses: gmliu@jmu.edu.cn (G. Liu), liuqingmei@jmu.edu.cn (Q. Liu).

https://doi.org/10.1016/j.fochx.2024.101613
Received 26 February 2024; Received in revised form 28 June 2024; Accepted 2 July 2024
Available online 6 July 2024

biological activities (Chen, Wang, Hong, et al., 2022; Luo et al., 2023). TPS, in particular, has antioxidant (Chen et al., 2018), immune-stimulating (Wang et al., 2019), and regulatory activities of intestinal flora (Chen, Wang, Zeng, et al., 2022). Due to its unique physical and chemical properties and structural characteristics, it has the potential to be developed as a functional food and has the potential to be used as a biofilm, drug carrier, and emulsifier in the medical field (Chen et al., 2016; Liu et al., 2022; Zhang et al., 2024). Furthermore, studies have shown that theanine, catechin, theaflavin, and other tea-derived compounds have anti-allergic properties by reducing immunoglobulin (Ig) E and histamine levels and decreasing FcεRI expression (Li et al., 2021). Since 1997, researchers have continuously discovered that various alginate polysaccharides, including alginic acid from seaweed, have anti-allergic effects by inhibiting hyaluronidase activity and histamine secretion in mast cells (Zhang et al., 2022). Similarly, polysaccharides derived from herbs have also been found to exhibit anti-allergic activity (Gao et al., 2018). Nevertheless, it remains unclear whether TPS has anti-allergic effect, and the effect of TPS on mast cells is yet to be determined.

Red-edge tea, a historical oolong tea variety cultivated extensively in Shaxian, China, was the focus in this study. The aim was to extract red-edge tea polysaccharide (RETPS) using hot water treatment and evaluate its mast cell stabilization activity. Since RETPS contained water-soluble impurities, additional purification steps were implemented. The physicochemical properties and mast cell stabilization activities of the polysaccharides before and after purification were analyzed.

2. Materials and methods

2.1. Materials and chemicals

Red-edge tea came from Fujian, China, and was purchased by Xiamen Sci-plus Biotech Co., Ltd. Cellulose DEAE-52 was obtained from Beijing Solarbio Science & Technology Co., Ltd. Glucuronic acid, glucose, 3,5-Dinitrosalicylic acid, and Kbr (Chromatographically pure) were obtained from Shanghai Macklin Biochemical Technology Co., Ltd. RBL-2H3 cells were purchased from Shanghai EK-Bioscience Biotechnology company. Cell counting kit-8 was provided by LABLEAD Inc. (Beijing, China). OVA, Evans blue, and anti-dinitrophenyl (DNP)-IgE were bought from Sigma (St Louis, MO, USA), and DNP-BSA was bought from Biosearch (Petaluma, CA, USA). Fetal bovine serum (FBS), trypsin 0.25% (1×) solution, and RPMI 1640 were purchased from Hyclone (Logan, UT, USA). ELISA kits of histamine and mouse mast cell proteinase (mMCP)-1 were purchased from Jiangsu Meimian Industrial Co., Ltd. (Jiangsu, China).

2.2. Extraction of RETPS

The dried tea leaves were powdered and then sieved through a 100-mesh screen. To remove the pigments and polyphenols from the RET samples, anhydrous ethanol was used three times at 55 °C for one hour each extraction. After drying, the precipitate is extracted three times with 80 °C water for one hour each time. The extract was then centrifuged and filtered to remove impurities, followed by precipitation with absolute ethanol. Crude RETPS was then obtained by centrifugation and lyophilization.

2.3. RBL-2H3 cell model

The RBL-2H3 cells were cultivated in a full RPMI-1640 medium supplemented with 10% FBS, 100 μg/mL streptomycin, and 100 U/mL penicillin. After that, the cells were kept in a humidified incubator with 5% CO_2 at 37 °C. Using CCK, the effects of different sample concentrations on RBL-2H3 cell viability were assessed.

The 0.1 μg/mL of anti-DNP-IgE was used to sensitize RBL-2H3 cells, and after 12 h, 5 μL polysaccharide solution with specified concentration was added to the culture hole, 1 h after sample intervention, 20 μg/mL of DNP-BSA was used to challenge these cells for 1 h. The control cells received identical volumes of vehicle control buffer. Cell supernatants and lysates were collected separately to measure β-hexosaminidase. And calculate β-hexosaminidase release according to the formula (2-1).

$$\beta-\text{hexosaminidase release}(\%)=\frac{\text{OD}_{405}\text{ of supernatant}}{(\text{OD}_{405}\text{ of supernatant}+\text{OD}_{405}\text{ of lysate})}\times 100\% \quad (2\text{-}1)$$

2.4. PCA model and PSA model

The Shanghai Laboratory Animal Center of the Chinese Academy of Sciences provided the female BALB/c mice, which were 6–8 weeks old and weighed 20 ± 2 g. The mice were kept in a specifically pathogen-free environment (SPF), with a 12-h light/dark cycle, a steady temperature of 22 ± 1 °C, and a relative humidity of 55 ± 10%. Food and drink were available to them at all times. The NIH guidelines (NIH Publication No. 85–23 Rev. 1985) for the use and care of laboratory animals were followed in the conduct of this investigation. All protocols were authorized by Jimei University's Animal Research Ethics Board (Xiamen, China; NO. SCXK 2016–0006).

The mice were put into groups at random after a week of acclimation. DNP-IgE (5 μg/mL for 100 μL) was injected intradermally into the left ear of each mouse. The polysaccharide solution was administered intragastrically for 200 μL after 24 h. Following an hour, the tail vein was punctured with an injection of 100 μL DNP-BSA (10 mg/mL Evans blue solution with 2 mg/mL of DNP-BSA). After 1 h, the left ears of the dizzy mice were photographed respectively, and after euthanasia by cervical dislocation, the left ear fragments were taken and incubated at 37 °C KOH for 12 h. Acetone and phosphoric acid were mixed according to 13:5 and added to the above system for neutralization reaction, then the absorbance of the supernatant was measured at 620 nm to quantify the amount of the dye in the mouse ear.

The mice were randomly divided into groups of five. An intravenous dose of 1.6 μg DNP-IgE in 200 μL was used to prime each mouse, and 24 h later, an injection of 750 μg DNP-BSA in 150 μL PBS was used to induce anaphylaxis. One hour before intravenous injection of DNP-BSA, the mice were intragastric administration of the polysaccharide solution for 200 μL. Following intravenous injection, the mice's anal temperature was taken every 10 min for the first hour, starting at minute 0. In PCA and PSA models, the control mice received identical volumes of vehicle control buffer.

2.5. Purification, molecular weight, and chemical composition analysis

To purify RETPS, a DEAE-52 cellulose column (3 cm × 40 cm) was used to filter the RETPS solution (100 mL, 30 mg/mL), which was then eluted stepwise at a flow rate of 2.0 mL/min using a series of gradient NaCl solutions (0.0, 0.1, 0.2, and 0.4 mol/L). An automatic collector was used to collect the eluate (6 mL /tube). The sulphuric acid-phenol

technique was used to calculate the polysaccharide content.

The phenol-sulphuric acid method was used to assess the total sugar content of RETPS, RETPS-1, RETPS-2, RETPS-3, and RETPS-4. The colorimetric method of 3,5-dinitro salicylic acid was used for the determination of reducing sugar content; the protein content was determined using a BCA protein detection kit. The carbazole-sulphuric acid method was used to determine uronic acid. Barium chloride turbidimetric method for the determination of sulfate content.

The gel chromatography difference multi-angle laser light scattering technique was utilized to ascertain the molecular weight of the polysaccharides. Thermo USA's U3000 liquid phase system and Wyatt Technology, CA, USA's Optilab T-rEX difference detector were used. The Wyatt Technology, CA, USA-based DAWN HELEOS II was the laser light scattering detector. Gel exclusion columns Ohpak SB-805 HQ (300 × 8 mm) and SB-803 HQ (300 × 8 mm) were used in sequence. The sample size was 100 μL, the mobile phase was A (0.02% NaN_3, 0.1 M $NaNO_3$), the flow rate was 0.6 mL/min, the elution gradient was 75 min, and the column temperature was 45 °C. After being dissolved in an aqueous solution of 0.1 M $NaNO_3$ (which included 0.02% NaN3, *w*/w) to a final concentration of 1 mg/mL, the sample was filtered through a 0.45 μm pore size filter and subjected to a machine assay. Technical support was provided by Sanshu Biotechnology. Co., Led. (Jiangsu, China).

2.6. Monosaccharide composition assays

Ion chromatography was used to determine the monosaccharide content of polysaccharides (ICS5000, Thermo Fisher Scientific Co., Ltd., MA, USA). After adding 1 mL of a 2 M trifluoroacetic acid (TFA) solution, the polysaccharide sample was heated to 121 °C for two hours, dried with nitrogen gas, cleaned with 99.99% methanol, and then dried once more. After dissolving the substance in sterile water, it was moved to a chromatographic vial for measurement. The monosaccharide component was found using a DionexTM CarboPacTM PA20 (150 × 3.0 mm, 10 μm) liquid chromatography column at a flow rate of 0.5 mL/min. The system temperature was set to 30 °C, and the injection volume was fixed at 5 μL. H_2O and 0.1 M NaOH, respectively, were the contents of mobile phases A and B; 0.1 M NaOH and 0.2 M NaAc made up mobile phase C.

2.7. Particle size and zeta potential analysis

RETPS, RETPS-1, RETPS-2, RETPS-3, and RETPS-4 sample solutions (2.5 mg/mL, 5 mg/mL, and 10 mg/mL) were subjected to zeta-potential and average particle size measurements using a Zetasizer nano ZS90 (Malvern Panalytical Technologies, England, UK).

2.8. Rheological analysis and scanning electron microscopy analysis

The apparent viscosity was measured using the DHR-2 Rheometer (TA Co., Newcastle, DE, USA). The rheometer was equipped with a 40 mm conical plate and the effects of different shear rates and shear concentrations on the viscosity of RETPS, RETPS-1, RETPS-2, RETPS-3, and RETPS-4 solutions were investigated. Double-sided tape was used to secure the solid sample to the side, and vacuum-sprayed gold was sputter-coated over it for 100 s. Employing a scanning electron microscope with thermal field emission (Phenom word Co., Eindhoven, The Netherlands).

2.9. Infrared spectrum analysis and circular dichroism spectroscopy analysis

The solid sample was crushed, combined in a 1:100 ratio with dried potassium bromide, and scanned at 400–4000 cm^{-1} using a Fourier infrared spectrometer after manually compressed. A spectropolarimeter was used to measure the circular dichroism (CD) spectroscopy of RETPS, RETPS-2, RETPS-3, and RETPS-4. The concentration of the sample was 2.0 mg/mL. Three scans of the CD spectra were conducted at a speed of 30 nm/min, covering a wavelength range of 190–260 nm.

2.10. Statistical analysis

The means ± SD were used to express all the values. One-way analysis of variance (ANOVA) was used for the statistical analysis, and Duncan's multiple-range test was used to assess the significance of the differences between the samples. GraphPad Prism and SPSS statistics 26 (SPSS INC., Chicago, IL, USA) were used for statistical analysis. The threshold for statistical significance was fixed at $P < 0.05$.

3. Results and discussion

3.1. Degranulation inhibition activity of RETPS in vitro

In the first step, we prepared RETPS and conducted an RBL-2H3 cell degranulation experiment to verify its stabilizing effect on mast cells. To assess RETPS's cytotoxicity, the CCK method was employed. At concentrations ranging from 25 to 100 μg/mL, RETPS exhibited no significant impact on RBL-2H3 cell viability, with cell viability consistently above 90% (Fig. 1A). Fig. 1B shows that RBL-2H3 cells underwent 17.95% β-hexosaminidase release rate without DNP-BSA treatment and 53.72% β-hexosaminidase release rate with DNP-BSA stimulation. These fingings suggest that both IgE intervention and DNP-BSA stimulation led to RBL-2H3 cell degranulation. However, upon intervention with RETPS, the release rate of β-hexosaminidase in RBL-2H3 cells significantly decreased, with the reduction correlating to the concentration of the sample. These results suggest that RETPS possesses anti-allergic potential by inhibiting mast cell degranulation.

RBL-2H3 cell degranulation models are commonly used to validate the anti-allergic properties of natural active ingredients. Allergens elicit a cytokinesis-mediated degranulation response in mast cells or basophils, with β-hexosaminidase serving as a biomarker of mast cell degranulation (Sahid & Kiyoi, 2020). As previously mentioned, RETPS inhibited β-hexosaminidase release in mast cells, suggesting that RETPS can stabilize mast cells by hindering the exocytosis process of RBL-2H3 cells.

3.2. Mast cell stabilization activity of RETPS in PCA and PSA model

PCA and PSA models were used to further investigate the impact of RETPS on mast cells in allergic organisms. In mouse passive allergic models, IgE is injected into mice and binds to FcεRI on mast cells to form a complex, and when BSA binds to this complex, mast cell degranulation will cause passive allergic reactions in mice (Bryce et al., 2016). In the PCA model, IgE combined with BSA triggered mast cell degranulation, leading to a cascade of reactions that resulted in increased vascular permeability and Evans blue dye extravasation in the ears of mice (Bryce et al., 2016). Consequently, the intensity of blue plaques on mouse ears served as an indicator of the extent of allergic reaction. As depicted in Fig. 2A, mice in the DNP-BSA group exhibited distinct blue spots throughout their ears compared to those in the PBS group, confirming the successful construction of the model and the noticeable differences between the negative and positive groups. Following the administration of RETPS injection, there was a considerable suppression of Evans blue extravasation from mouse ears. Moreover, the degree of extravasation decreased progressively with increasing concentrations of RETPS, indicating a concentration-dependent suppression of PCA in mice. The quantitative analysis of dye extravasation in Fig. 2B demonstrated that the content of Evans blue in the left ear of the DNP-BSA group was substantially higher than that of the PBS group. Conversely, in the RETPS intervention group, the amount of Evans blue in the left ear decreased considerably in a concentration-dependent manner compared to the DNP-BSA group. Similar to the study of Han et al. (Han et al., 2020), these findings strongly suggest that RETPS exhibits *in vivo* mast

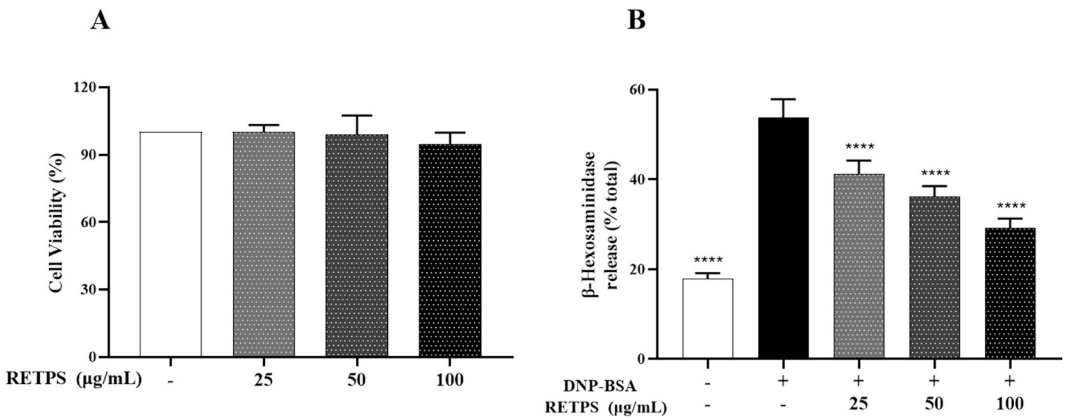

Fig. 1. Effects of RETPS on the viability (A) and the release of β-hexosaminidase (B) of RBL-2H3 cells. Values were presented as mean ± SD (n = 4), ****$P < 0.0001$ *vs* DNP-BSA group.

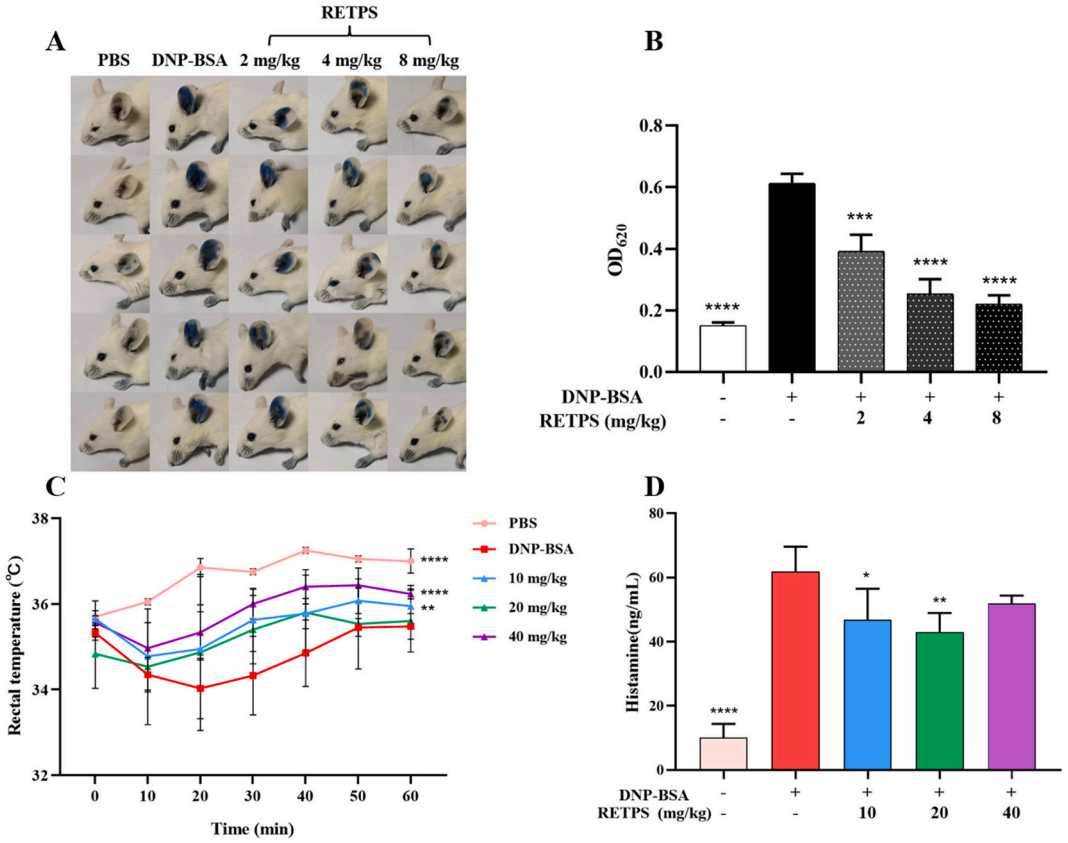

Fig. 2. Effects of RETPS on IgE/BSA-induced PCA and PSA reaction.
(A) The ears of mice that had absorbed Evans blue were photographed; (B) Evans blue extraction of mice ear fragments. (C) The rectal temperature of mice within one hour after BSA injection; (D) Histamine content in serum of mice. Values were presented as mean ± SD (n = 5), * $P < 0.05$, ** $P < 0.01$, *** $P < 0.01$, ****$P < 0.0001$ *vs* DNP-BSA group. (For interpretation of the references to colour in this figure legend, the reader is referred to the web version of this article.)

cell stabilizing properties.

The experimental obtained from the PCA model solely reflects local effects, while food allergy can cause multi-organ or even systemic reactions (Renz et al., 2018). Therefore, in order to further validate the efficacy of RETPS, the PSA model was used as the evaluation criterion. Sensitization of mice was achieved by injecting DNP-IgE into the tail vein, followed by the administration of DNP-BSA *via* the venous blood vessels after a 24-h interval. The occurrence of systemic anaphylaxis in mice was expressed by monitoring rectal body temperature. In the PSA model, IgE and BSA induce systemic allergic reactions in mice, primarily manifested as a decrease in body temperature (Kulinski et al., 2018). As shown in Fig. 2C, mice in the PBS group consistently maintained rectal temperatures above 36 °C, whereas those injected with DNP-BSA experienced a sharp temperature drop by the tenth minute. Conversely, mice treated with RETPS exhibited elevated body temperatures compared to the DNP-BSA group. The temperature increase was observed at the 30th minute for mice in the DNP-BSA group, while mice in the RETPS groups showed an increase at the 20th minute. In order to determine whether RETPS could influence mast cell stabilization, histamine levels, a biomarker of mast cell degranulation, were evaluated

(Fig. 2D). The serum histamine content in the PBS group was below 20 ng/mL, whereas it exceeded 60 ng/mL in the DNP-BSA group, indicating the induction of mast cell degranulation *in vivo* in response to PSA. Mice treated with RETPS showed lower histamine levels compared to those in the DNP-BSA group. However, this inhibition did not exhibit a significant concentration dependence, possibly due to the short half-life of histamine, resulting in its loss during the detection process. Nevertheless, these findings suggest that RETPS may exert an anti-allergic effect on mice by maintaining mast cell stability.

RETPS exhibited mast cell stabilization activity both *in vitro* and *in vivo*. However, since RETPS is a crude extract containing some water-soluble impurities, it was necessary to purify it to validate that the aforementioned antiallergic activity was indeed derived from the polysaccharide component. Thus, the properties and activities of different components were compared.

3.3. Molecular weight, chemical composition, and monosaccharide composition of polysaccharides

Cellulose DEAE-52 is a widely used filler for the separation and purification of polysaccharides (Liu et al., 2022). As shown in Fig. S1, four polysaccharide fractions eluted by 0.0, 0.1, 0.2, and 0.4 mol/L NaCl were obtained, which were named RETPS-1, RETPS-2, RETPS-3, and RETPS-4, respectively. The yields of RETPS-1, RETPS-2, RETPS-3, and RETPS-4, were 24.60%, 3.50%, 8.60% and 6.87%, respectively. It is worth noting that after purification, the total polysaccharide extraction rate was 43.57% (calculated according to the yield of RETPS-1, RETPS-2, RETPS-3, and RETPS-4). The low yield may be due to the following three reasons: (1) Some free proteins of large molecules in RETPS remain on the purification column; (2) The low molecular weight sugars in RETPS-1 were lost during dialysis; (3) The recovery process after lyophilization will lose some polysaccharides.

Based on the chemical composition analysis presented in Table 1, it is evident that RETPS exhibits the lowest total sugar and reducing sugar content, as well as the highest molecular weight. Additionally, it exhibits the highest protein content, indicating the elimination of water-soluble free proteins and some impurities during the purification process. It has been reported that there is considerable variation in the total sugar content of TPS derived from different parts of the tea tree. Furthermore, it is noteworthy that each purified component contains proteins, indicating the potential presence of glycoproteins conjugated with proteins within the polysaccharide (Xiang et al., 2023). To confirm this view, the crude polysaccharide was deproteinized *via* the Sevag technique, and following dialysis lyophilization, it was purified. The protein content of each purified component was not significantly different from the directly pure polysaccharide without Sevag treatment. However, this treatment would result in a larger loss of polysaccharides. As a result, no deproteinization was carried out in the studies that followed. The uronic acid content of RETPS-3 and RETPS-4 was significantly higher than that of RETPS ($P < 0.05$), which is consistent with the monosaccharide composition results. According to a report, uronic acid is a prominent component of tea polysaccharides with the potential to exert anti-allergic activity (Wang et al., 2015). Notably, all samples were found to contain sulfate moieties, an acidic group that may contribute to the anti-allergic activity of tea polysaccharides (Li et al., 2023). In addition, the chemical composition of polysaccharides is detected according to the colour reaction of chemical groups, and RETPS contain some water-soluble pigments, so the measured value is greater than the actual value, and the total sugar, protein, and sulfate percentage of RETPS can be added up to >100%. However, for RETPS-1, a small molecular mixture of sugars and water-soluble impurities, at the same concentration, the chemical composition of polysaccharides is lower than other purified components.

The monosaccharide composition of RETPSs is shown in Table 2. Similar to other previous results, RETPS consists of 8 monosaccharides (Zhang et al., 2024). The main components of RETPS, RETPS-1, and RETPS-2 were arabinose, galactose, and glucose, while the main components of RETPS-3 and RETPS-4 were arabinose, galactose, and galacturonic acid. In comparison to RETPS, the glucose content of RETPS-3 and RETPS-4 exhibited a significant reduction, accompanied by a substantial increase in Gal-UA content. This phenomenon can be attributed to the anion exchange purification principle employed by the DEAE cellulose column. During the purification process, non-acidic sugars are eliminated through washing steps, whereas acidic sugars become enriched in the elution components with high NaCl concentration (Liao et al., 2022).

The analysis of particle size for the polysaccharide was conducted. As shown in Table S1, the particle size of each polysaccharide demonstrates an increase with the rise in solution concentration. It should be noted that a reduction in electrostatic repulsion between droplets in a polysaccharide solution promotes flocculation, leading to an increase in the mean particle size (Griffin & Khouryieh, 2020). Compared with RETPS, the particle size of the purified polysaccharide was larger at the same concentration, indicating that the electrostatic repulsion between the purified component droplets was smaller.

3.4. Zeta potential, dynamic viscosity, and microstructure of polysaccharides

In aqueous solutions, the zeta potential reflects the dissociation of ions on the surface of the particle and can characterize the stability of the dispersive system (Cano-Sarmiento et al., 2018). To eliminate the influence of salt ions on the zeta potential, dialysis treatment was employed. Fig. 3A presents the zeta potential values for RETPS, RETPS-1, RETPS-2, RETPS-3, and RETPS-4. The absolute Zeta potential of RETPS and RETPS-1 showed a decreasing trend with increasing

Table 1
The molecular weight and chemical composition of RETPS, RETPS-1, RETPS-2, RETPS-3, and RETPS-4.

Sample	RETPS	RETPS-1	RETPS-2	RETPS-3	RETPS-4
Mw (kDa)	310.54	28.62	27.41	106.61	53.95
Total sugar (%)	35.43 ± 0.61^{d}	23.33 ± 0.80^{e}	61.59 ± 0.55^{a}	49.28 ± 0.52^{c}	55.13 ± 0.13^{b}
Reducing sugar (%)	12.86 ± 0.59^{b}	5.02 ± 0.26^{c}	17.82 ± 1.20^{a}	4.69 ± 0.63^{c}	6.32 ± 0.50^{c}
Protein (%)	57.53 ± 3.01^{a}	16.04 ± 0.71^{bc}	14.91 ± 0.65^{c}	13.05 ± 0.27^{c}	20.82 ± 1.26^{b}
Uronic acid (%)	15.26 ± 0.42^{d}	5.72 ± 0.11^{e}	39.92 ± 2.28^{c}	58.87 ± 2.22^{b}	47.05 ± 0.86^{a}
Sulfate (%)	20.16 ± 2.83^{a}	7.80 ± 1.01^{c}	12.00 ± 1.07^{b}	12.46 ± 2.55^{b}	16.02 ± 3.15^{ab}

Mw: Molecular weight. Values are expressed as means ± SD and three replicated independent determinations; Values with different letters in the same line indicate statistically significant differences ($P < 0.05$).

Table 2
The monosaccharide composition of RETPS, RETPS-1, RETPS-2, RETPS-3, and RETPS-4.

Sample	RETPS	RETPS-1	RETPS-2	RETPS-3	RETPS-4
Fucose (%)	ND	ND	ND	ND	ND
Rhamnose (%)	4.82	ND	3.81	7.92	11.34
Arabinose (%)	18.94	16.82	19.06	23.94	26.49
Galactose (%)	22.35	19.65	26.05	21.61	24.58
Glucose (%)	36.17	55.12	37.61	5.05	6.24
Xylose (%)	3.78	1.52	2.00	2.14	3.83
Mannose (%)	2.40	6.89	4.53	2.53	4.05
Fructose (%)	ND	ND	ND	ND	ND
Ribose (%)	ND	ND	ND	ND	ND
Galacturonic Acid (%)	9.65	ND	4.63	34.11	20.57
Guluronic Acid (%)	ND	ND	ND	ND	ND
Glucuronic Acid (%)	1.89	ND	2.31	2.69	2.89
Mannuronic Acid (%)	ND	ND	ND	ND	ND

ND, non-detectable, or lower than the limit of quantification.

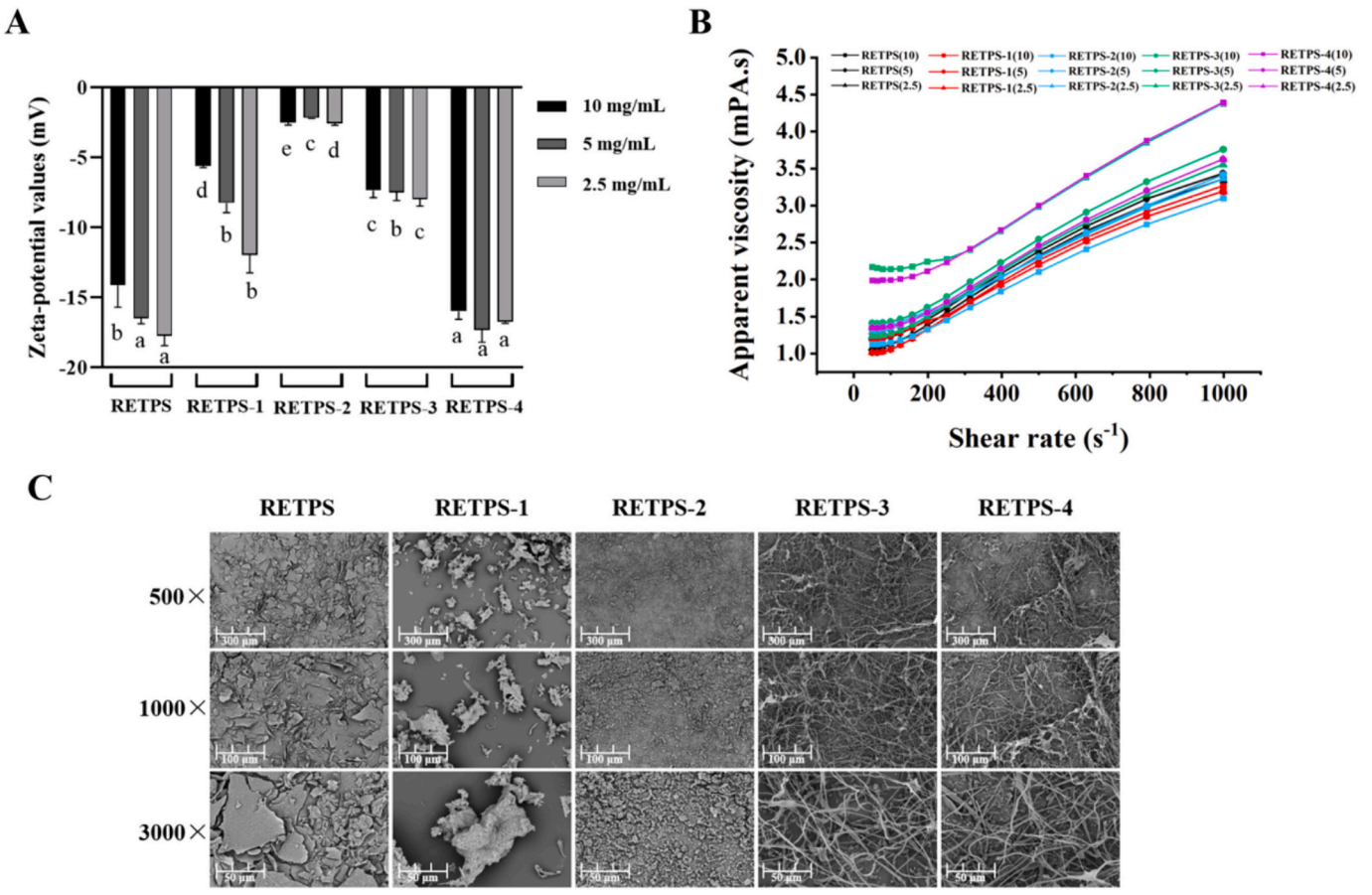

Fig. 3. The Zeta potential (A), apparent viscosity (B), and microstructure (C) of RETPS, RETPS-1, RETPS-2, RETPS-3, and RETPS-4.
(A) The Zeta potential of RETPS, RETPS-1, RETPS-2, RETPS-3, and RETPS-4, Values with different letters in the same concentration indicate statistically significant differences; (B) The apparent viscosity of RETPS, RETPS-1, RETPS-2, RETPS-3, and RETPS-4 at different concentrations for the shear rates in the range of 50–1000 s^{-1}. RETPS, RETPS-1, RETPS-2, RETPS-3, and RETPS-4 were dissolved in ultrapure water with various concentrations of 2.5 mg/mL, 5 mg/mL, and 10 mg/mL; (C) Scanning electron micrographs of RETPS, RETPS-1, RETPS-2, RETPS-3, and RETPS-4 at different Magnifications (500×, 1000×, 3000×).

concentration, which may be attributed to the decrease of electrostatic repulsion and interfacial film strength between the solutes with increasing concentration, increasing droplet size, and decrease of emulsion stability (Han et al., 2022). On the other hand, the absolute Zeta potentials of the RETPS-2, RETPS-3, and RETPS-4 groups did not show any significant difference with solution concentration. This indicates that RETPS-1, RETPS-2, RETPS-3, and RETPS-4 possess a higher level of homogeneity compared to RETPS. A larger absolute value of the zeta potential indicates that the dispersive system is more stable, so in general, RETPS-4 exhibits the best stability (S. Wang et al., 2020).

The viscosity of the samples at different concentrations (2.5 mg/mL, 5 mg/mL, and 10 mg/mL) varied with the shear rates (50–1000 s^{-1}), as shown in Fig. 3B. The apparent viscosity of protein/polysaccharide condensates is determined by electrostatic interactions (Niu et al., 2018). The stronger the electrostatic interaction, the higher the apparent viscosity and the easier it is to form aggregates (Mao et al., 2023). The formation of new hydrogen bonds between polysaccharide network structures can promote the formation of more dense gel, and thus increase the viscosity of polysaccharide solution (Tao et al., 2022). RETPS and its purified groups are protein-polysaccharide condensates, at high concentrations, the viscosity of RETPS-3 and RETPS-4 is greater than that of the remaining components, indicating that the solution of RETPS-3 and RETPS-4 had stronger electrostatic interaction and a new hydrogen bond may have been formed between polysaccharide macromolecules in the solution. In addition, the apparent viscosities of all the samples increase with increasing shear rate, which is a typical characteristic of non-Newtonian liquids. This suggests that the red-edge tea polysaccharides may have shorter main chains and abundant branched chains. Initially, the apparent viscosity was primarily influenced by the entanglement of the main chain at lower shear rates. However, due to the shorter main chains, the intermolecular entanglement was rapidly disrupted, resulting in minimal viscosity changes. Nevertheless, as the shear rate increased, the molecules continued to aggregate, leading to more frequent particle collisions and increased entanglement of the branched chains. Consequently, the apparent viscosity of the different polysaccharide groups increased (Ma et al., 2017). Eventually, the apparent viscosity of red-border tea polysaccharides exhibited a gradual increase once again. Meanwhile, because the average molecular weight and viscosity of these polysaccharide solutions are beyond the detection range of conventional instruments, it's difficult to conduct further structural analysis of them.

Fig. 3C shows that the microstructure of RETPS is flaky with a rough and cracked surface, and numerous pores in the internal structure. RETPS-1 showed irregularly curled flakes with rough and cracked surfaces when magnified 3000 times. The microstructure of RETPS-2 is lamellar, with a complete structure and smooth and dense surface. RETPS-3 and RETPS-4 were irregularly curled with smooth and dense surfaces. The removal of unstable substances bound to the polysaccharide by NaCl elution may have caused changes in the microscopic morphology of the polysaccharide samples (Fan et al., 2018). Overall, displays greater homogeneity, aligning with the findings from the zeta potential determination.

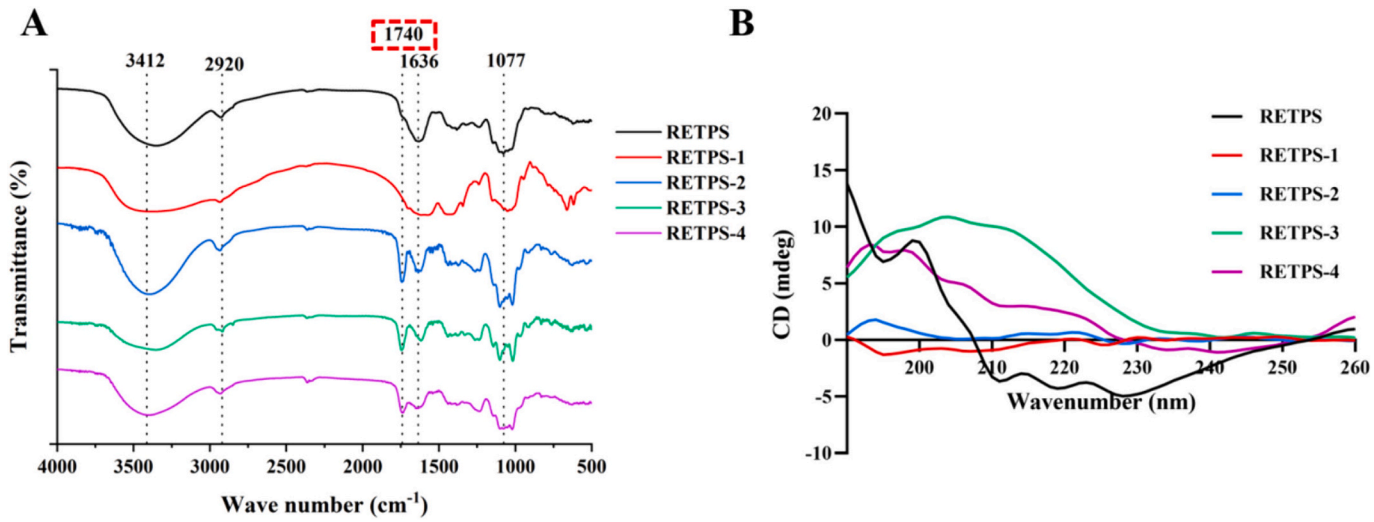

Fig. 4. Infrared spectrum (A) and circular dichroism spectra (B) of RETPS, RETPS-1, RETPS-2, RETPS-3, and RETPS-4.

3.5. Functional groups and secondary structure of polysaccharides

The infrared spectrum of RETPS, RETPS-1, RETPS-2, RETPS-3, and RETPS-4 were analyzed (Fig. 4A). The characteristic band area 3412 cm^{-1} corresponds to the O—H stretching vibration present in all RETPS samples. The absorption peak at 2920 cm^{-1} indicates the C—H stretching vibration, which is typical of polysaccharides (Yuan et al., 2015). The absorption peak at 1636 cm^{-1} is characteristic of C═O absorption (Olennikov et al., 2015). The presence of pyranose galactose in the main chain is indicated by the absorption at 1077 cm^{-1} (Zhao et al., 2014). Notably, RETPS-2, RETPS-3, and RETPS-4 exhibit distinct absorption peaks at 1740 cm^{-1}, which are characteristic of free acid tincture (Wang et al., 2012). This suggests that NaCl elution removes impurities and exposes the acidic groups of polysaccharides. These results demonstrate that all RETPS samples exhibit typical polysaccharide infrared spectrum absorption peaks.

Previous studies have shown that tea polysaccharide is a polysaccharide and protein conjugate (Zhang et al., 2024), so in this study, CD spectroscopy was performed on RETPS, and each purified component. As shown in Fig. 4B, RETPS exhibited a positive Cotton effect in the wavelength range of 190 nm to 208 nm, followed by a negative Cotton effect from 208 nm to 250 nm. A positive-negative crossover at 205 nm, corresponds to α-helix conformation (Micsonai et al., 2023). RETPS-3 and RETPS-4 showed a positive Cotton effect in wavelengths of 190–230 nm, which correspond to α-helix and β-turn proteins, respectively. However, there is no corresponding negative Cotton effect, indicating an irregular secondary structure for RETPS-3 and RETPS-4. These proteins may be inherently disordered, consisting of residues that do not adopt helical or sheet-like structures. These irregular proteins may have crucial roles in molecular recognition and signaling in various biological processes (Miles et al., 2023), so the anti-allergic effect of RETPS-3 and RETPS-4 may also be related to their unique protein structure.

3.6. Degranulation inhibition activity of purified RETPS components in vitro

RETPS is a crude extract that contains some water-soluble impurities. To further confirm that the observed activity is indeed derived from polysaccharides, we used RBL-2H3 cells to verify the activities of

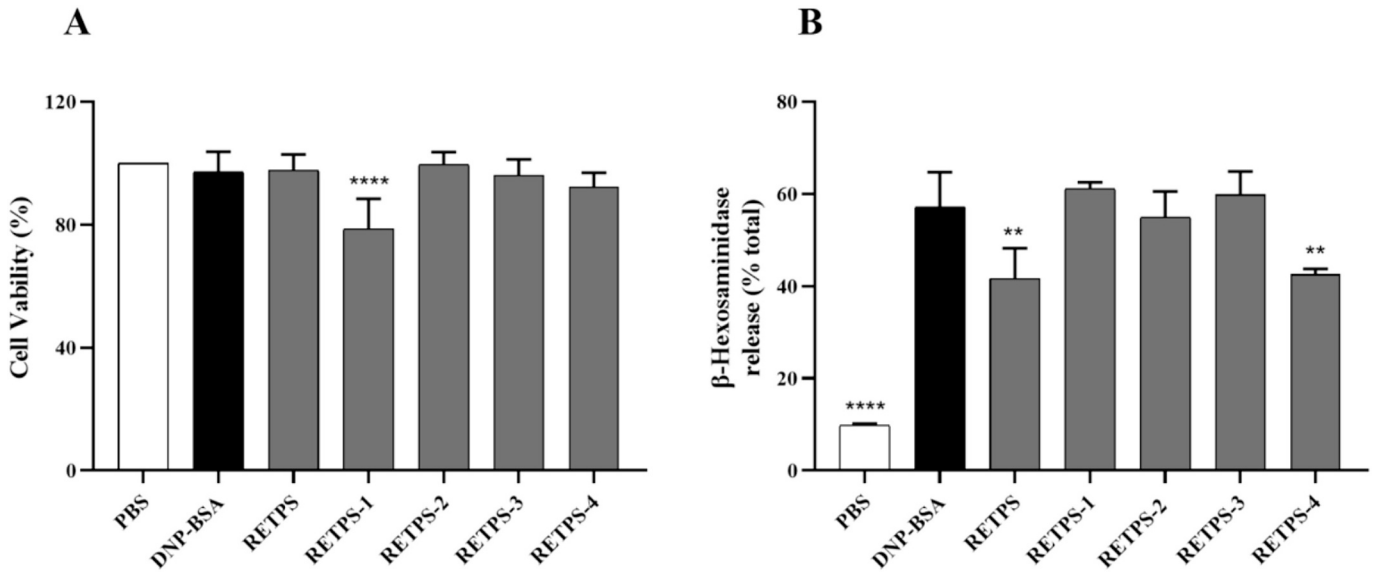

Fig. 5. Effects of RETPS on the viability (A) and the release of β-hexosaminidase (B) of RBL-2H3 cells, when the concentration is 100 μg/mL. Values were presented as mean ± SD ($n = 4$), $^{****}P < 0.0001$ *vs* DNP-BSA group.

purified polysaccharides. As shown in Fig. 5A, RETPS, RETPS-2, RETPS-3, and RETPS-4 were not cytotoxic to RBL-2H3 cells at a concentration of 100 μg/mL, whereas RETPS-1 significantly reduced the viability of RBL-2H3 cells. This suggests that cell-harmful substances are enriched in RETPS-1. In Fig. 5B, the release rate of β-hexosaminidase of RBL-2H3 cells was 14.73% in the PBS group, and it reached 68.89% in the BSA group. After intervention with RETPS and RETPS-4, the efficiency of releasing β-hexosaminidase in RBL-2H3 cells was significantly reduced. This indicats that RETPS and RETPS-4 could inhibit mast cell degranulation.

3.7. Mast cell stabilization activity of purified RETPS components in PCA and PSA model

Next, the PCA model was used to assess the differences in activity among the different components of RETPS. As shown in Fig. 6A, all four polysaccharides inhibited the blue dye extravasation from mouse ears at the action concentration of 4 mg/kg compared with DNP-BSA group. Based on the quantitative results of dye extravasation in Fig. 6B, the anti-allergic activities of the four polysaccharides were ranked as RETPS-4 ≈ RETPS-3 > RETPS > RETPS-2. Unlike the results of the cell experiments, RETPS-3 showed a better effect than RETPS in the PCA model. This may be due to RETTS-3 being difficult to enter the cell *in vitro* experiment, as it can be absorbed by the intestinal cell following digestion and degradation in the gastrointestinal tract to exert a biological role *in vivo*.

The PSA model was utilized to further verify the anti-allergic effects of different components of RETPS on mice. Due to the low yield of RETPS-2 and the PCA experiment results indicating its inferior anti-allergic activity to RETPS, only RETPS, RETPS-3, and RETPS-4 were selected for comparison to reduce the number of experimental animals. As shown in Fig. 6C, when the dose concentration was 20 mg/kg, compared with the DNP-BSA group, all three polysaccharides exhibited the ability to inhibit hypothermia in mice, with RETPS-3, RETPS-4, and RETPS demonstrating anti-allergic activities in that order. Since mast cells are the primary effector cells in food allergic reactions, the mMCP-1 content in mice's serum was measured. As shown in Fig. 6D, RETPS-3 and RETPS-4 had the most pronounced effect in stabilizing mast cells, followed by RETPS. Slight deviations in body temperature may be attributed to experimental error. In general, the aforementioned experiments have proved that polysaccharides are the constituents responsible for exerting mast cell stabilization activity.

Polysaccharides are macromolecular substances that primarily enter cells through endocytosis *in vitro* cell experiments (Weber et al., 2019).

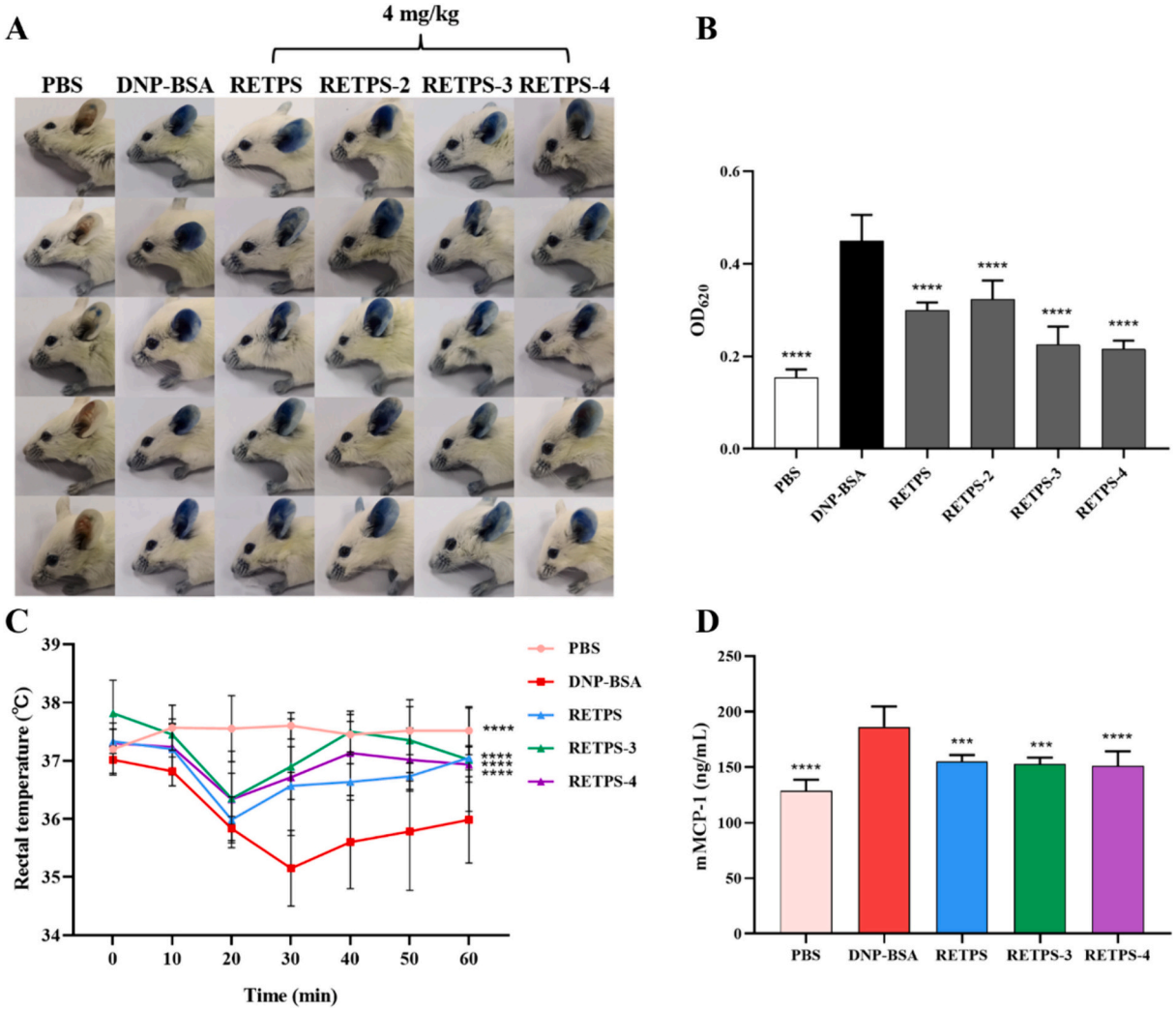

Fig. 6. Effects of RETPS, RETPS-2, RETPS-3, and RETPS-4 on IgE/BSA-induced PCA and PSA reaction. (A) The ears of mice that had absorbed Evans blue were photographed; (B)Evans blue extraction of mice ear fragments. (C) The rectal temperature of mice within one hour after BSA injection; (D) mMCP-1 content in serum of mice. The concentration of samples in the PCA model is 4 mg/kg, and the concentration of samples in the PSA model is 20 mg/kg. Values were presented as mean ± SD ($n = 5$), *** $P < 0.001$, ****$P < 0.0001$ *vs* DNP-BSA group. (For interpretation of the references to colour in this figure legend, the reader is referred to the web version of this article.)

In *in vivo* experiments, orally administered polysaccharides undergo digestion and degradation in gastric fluid before being absorbed and utilized by the intestine. Factors such as charge, Mw, spatial structure, and dosage are the main determinants of the amount of polysaccharides absorbed (Zheng et al., 2022). Consequently, the biological activity of polysaccharides may differ between *in vivo* and *in vitro* experiments. This implies the need for further research to comprehend the functional mechanisms of the aforementioned polysaccharides in organisms. Proteases, which are the primary proteins present in mast cell granules, serve as pharmacological targets for allergic reactions involving activated cell. They are extensively employed in the study of allergen sensitization and anti-allergy drugs (Liu et al., 2024). Hence, the reduction of serum mMCP-1 content in mice in PSA tests can also indicate that the tested sample has the potential to exert an anti-allergic role by stabilizing mast cells. In addition, it has been reported that tea polysaccharides can participate in the regulation of intestinal flora structure after being degraded by intestinal flora in organisms (Tan et al., 2023), and the metabolites after bacterial degradation may have anti-inflammatory activities (Chen, Wang, Hong, et al., 2022; Chen, Wang, Zeng, et al., 2022). Therefore, in the follow-up analysis of the *in vivo* antiallergic activity of RETPS-3 and RETPS-4, we will explore the interaction between these two components and intestinal flora. In recent years, structure-function relationships of protein-polysaccharide mixtures have been extensively studied, such as nanoparticles, molecular couplings, hydrogels, and edible membranes obtained by forming aggregation complexes (Wahyu Wijaya, 2017). As a natural glycoprotein conjugate, RETPS-3 and RETPS-4 have broad application potential in the field of anti-allergic functional food.

4. Conclusion

This study revealed that RETPS effectively reduced the degranulation of RBL-2H3 cells and alleviated symptoms accociated with mast cell-mediated PCA and PSA reaction. To confirm the polysaccharide's contribution to this activity, the crude polysaccharide underwent purification. RETPS-3 and RETPS-4 exhibited decreased solubility, increased apparent viscosity, and reduced molecular weight compared to RETPS. Additionally, their microstructure appeared denser and smoother while the secondary structure of the protein became irregular. Monosaccharide composition analysis indicated that RETPS primarily consists of arabinose, galactose, and glucose, whereas RETPS-3 and RETPS-4 are predominantly composed of arabinose, galactose, and galacturonic acid. Moreover, RETPS-3 and RETPS-4 exhibited superior *in vivo* activity compared to RETPS. In summary, polysaccharides derived from red-edge tea displayed significant anti-allergic activity. By employing purification and elution processes, it is possible to reduce glucose content and molecular weight in RETPS while increasing the concentration of galacturonic acid without compromising the main chain structure or sulfate groups. This phenomenon may accounts for the notably enhanced mast cell stability maintenance observed in RETPS-3 and RETPS-4. As a result, this study provides a promise theoretical foundation for the development of functional anti-allergic food products containing tea polysaccharides.

CRediT authorship contribution statement

Yan Li: Writing – review & editing, Writing – original draft, Methodology, Investigation, Data curation, Conceptualization. **Jinhao Pang:** Writing – review & editing, Validation, Supervision. **Yongfeng Lin:** Writing – review & editing, Validation, Supervision. **Wenmei Liu:** Writing – review & editing, Supervision, Resources. **Zehua Zou:** Writing – review & editing, Supervision, Resources. **Guangming Liu:** Writing – review & editing, Visualization, Project administration, Funding acquisition, Data curation. **Qingmei Liu:** Writing – review & editing, Visualization, Project administration, Funding acquisition, Data curation.

Declaration of competing interest

The authors declare that they have no known competing financial interests or personal relationships that could have appeared to influence the work reported in this paper.

Data availability

Data will be made available on request.

Acknowledgment

The following organizations provided funding for this work: National Natural Science Foundation of China (grant numbers: 32001695, 32072336, Fujian Science and Technology Project (award number: 2021L3013), and Sanming Science and Technology Project (project number: 2022-N-12).

Appendix A. Supplementary data

Supplementary data to this article can be found online at https://doi.org/10.1016/j.fochx.2024.101613.

References

Berin, M. C. (2023). Targeting type 2 immunity and the future of food allergy treatment. *The Journal of Experimental Medicine, 220*(4). https://doi.org/10.1084/jem.20221104

Bryce, P. J., Falahati, R., Kenney, L. L., Leung, J., Bebbington, C., Tomasevic, N., & Brehm, M. A. (2016). Humanized mouse model of mast cell–mediated passive cutaneous anaphylaxis and passive systemic anaphylaxis. *Journal of Allergy and Clinical Immunology, 138*(3), 769–779. https://doi.org/10.1016/j.jaci.2016.01.049

Cano-Sarmiento, C., Téllez-Medina, D. I., Viveros-Contreras, R., Cornejo-Mazón, M., Figueroa-Hernández, C. Y., García-Armenta, E., & Gutiérrez-López, G. F. (2018). Zeta potential of food matrices. *Food Engineering Reviews, 10*(3), 113–138. https://doi.org/10.1007/s12393-018-9176-z

Chen, C., Wang, H., Hong, T., Huang, X., Xia, S., Zhang, Y., & Nie, S. (2022). Effects of tea polysaccharides in combination with polyphenols on dextran sodium sulfate-induced colitis in mice. *Food Chemistry: X, 13*, Article 100190. https://doi.org/10.1016/j.fochx.2021.100190

Chen, G., Wang, M., Xie, M., Wan, P., Chen, D., Hu, B., & Liu, Z. (2018). Evaluation of chemical property, cytotoxicity and antioxidant activity in vitro and in vivo of polysaccharides from Fuzhuan brick teas. *International Journal of Biological Macromolecules, 116*, 120–127. https://doi.org/10.1016/j.ijbiomac.2018.04.184

Chen, G., Wang, M., Zeng, Z., Xie, M., Xu, W., Peng, Y., & Liu, Z. (2022). Fuzhuan brick tea polysaccharides serve as a promising candidate for remodeling the gut microbiota from colitis subjects in vitro: Fermentation characteristic and anti-inflammatory activity. *Food Chemistry, 391*, Article 133203. https://doi.org/10.1016/j.foodchem.2022.133203

Chen, G., Yuan, Q., Saeeduddin, M., Ou, S., Zeng, X., & Ye, H. (2016). Recent advances in tea polysaccharides: Extraction, purification, physicochemical characterization and bioactivities. *Carbohydrate Polymers, 153*, 663–678. https://doi.org/10.1016/j.carbpol.2016.08.022

Fan, M., Sun, X., Qian, Y., Xu, Y., Wang, D., & Cao, Y. (2018). Effects of metal ions in tea polysaccharides on their in vitro antioxidant activity and hypoglycemic activity. *International Journal of Biological Macromolecules, 113*, 418–426. https://doi.org/10.1016/j.ijbiomac.2018.01.041

Gao, Y., Jiang, Y., Chen, G., Li, S., Yang, F., & Ma, Q. (2018). A sensitive and rapid UPLC-MS/MS method for determination of monosaccharides and anti-allergic effect of the polysaccharides extracted from Saposhnikoviae Radix. *Molecules, 23*(8), 1924. https://doi.org/10.3390/molecules23081924

Griffin, K., & Khouryieh, H. (2020). Influence of electrostatic interactions on the formation and stability of multilayer fish oil-in-water emulsions stabilized by whey protein-xanthan-locust bean complexes. *Journal of Food Engineering, 277*, Article 109893. https://doi.org/10.1016/j.jfoodeng.2019.109893

Han, D., Mao, J., Zhao, J., Zhang, H., Wang, D., Wang, C., & Fu, M. (2022). Dissipative particle dynamics simulation and experimental analysis of the effect of anionic/cationic mixed surfactants on the stability of emulsions. *Journal of Molecular Liquids, 367*, Article 120482. https://doi.org/10.1016/j.molliq.2022.120482

Han, E. J., Kim, H., Sanjeewa, K. K. A., Jung, K., Jee, Y., Jeon, Y., & Ahn, G. (2020). Sargassum horneri as a functional food ameliorated IgE/BSA-induced mast cell activation and passive cutaneous anaphylaxis in mice. *Marine Drugs, 18*(12), 594. https://doi.org/10.3390/md18120594

Kulinski, J. M., Proia, R. L., Larson, E. M., Metcalfe, D. D., & Olivera, A. (2018). $S1P_4$ regulates passive systemic anaphylaxis in mice but is dispensable for canonical IgE-mediated responses in mast cells. *International Journal of Molecular Sciences, 19*(5), 1279. https://doi.org/10.3390/ijms19051279

Li, C., Tian, Y., Pei, J., Zhang, Y., Hao, D., Han, T., & Wang, Z. (2023). Sea cucumber chondroitin sulfate polysaccharides attenuate OVA-induced food allergy in BALB/c mice associated with gut microbiota metabolism and Treg cell differentiation. *Food & Function, 14*(16), 7375–7386. https://doi.org/10.1039/d3fo00146f

Li, Q., Wang, Y., Liang, Y., & Lu, J. (2021). The anti-allergic potential of tea: A review of its components, mechanisms and risks. *Food & Function, 12*(1), 57–69. https://doi.org/10.1039/d0fo02091e

Liao, Q., Pang, L., Li, J., Zhang, C., Li, J., Zhang, X., & Zhang, J. (2022). Characterization and diabetic wound healing benefits of protein-polysaccharide complexes isolated from an animal ethno-medicine *Periplaneta americana* L. *International Journal of Biological Macromolecules, 195*, 466–474. https://doi.org/10.1016/j.ijbiomac.2021.12.018

Liu, M., Gong, Z., Liu, H., Wang, J., Wang, D., Yang, Y., & Zhong, S. (2022). Structural characterization and anti-tumor activity in vitro of a water-soluble polysaccharide from dark brick tea. *International Journal of Biological Macromolecules, 205*, 615–625. https://doi.org/10.1016/j.ijbiomac.2022.02.089

Liu, Q., Zhang, Y., Shu, Z., Liu, M., Zeng, R., Wang, Y., & Liu, G. (2020). Sulfated oligosaccharide of Gracilaria lemaneiformis protect against food allergic response in mice by up-regulating immunosuppression. *Carbohydrate Polymers, 230*, Article 115567. https://doi.org/10.1016/j.carbpol.2019.115567

Liu, Y., Lin, S., Liu, K., Wang, S., Li, W., & Sun, N. (2024). Insights into sensitizing and eliciting capacity of gastric and gastrointestinal digestion products of shrimp (*Penaeus vannamei*) proteins in BALB/c mice. *Food Science and Human Wellness, 13*(1), 339–348. https://doi.org/10.26599/FSHW.2022.9250028

Luo, Q., Luo, L., Zhao, J., Wang, Y., & Luo, H. (2023). Biological potential and mechanisms of Tea's bioactive compounds: An updated review. *Journal of Advanced Research*. https://doi.org/10.1016/j.jare.2023.12.004

Ma, F., Zhang, Y., Liu, N., Zhang, J., Tan, G., Kannan, B., & Bell, A. E. (2017). Rheological properties of polysaccharides from Dioscorea opposita Thunb. *Food Chemistry, 227*, 64–72. https://doi.org/10.1016/j.foodchem.2017.01.072

Mao, Y., Huang, M., Bi, J., Sun, D., Li, H., & Yang, H. (2023). Effects of kappa-carrageenan on egg white ovalbumin for enhancing the gelation and rheological properties via electrostatic interactions. *Food Hydrocolloids, 134*, Article 108031. https://doi.org/10.1016/j.foodhyd.2022.108031

Micsonai, A., Moussong, É., Wien, F., Boros, E., Vadászi, H., Murvai, N., & Kardos, J. (2023). Bestsel: Updated webserver for secondary structure and fold prediction for protein CD spectroscopy. *Biophysical Journal, 122*(3, Supplement 1), Article 179a. https://doi.org/10.1016/j.bpj.2022.11.1110

Miles, A. J., Drew, E. D., & Wallace, B. A. (2023). DichroIDP: A method for analyses of intrinsically disordered proteins using circular dichroism spectroscopy. *Communications Biology, 6*(1), 823. https://doi.org/10.1038/s42003-023-05178-2

Nakajima, S., Manita, S., Yu, G., Ishimaru, K., Kono, K., Kitamura, K., & Nakao, A. (2020). Activation of the reward system ameliorates passive cutaneous anaphylactic reaction in mice. *Allergy (Copenhagen), 75*(12), 3275–3279. https://doi.org/10.1111/all.14442

Niu, F., Kou, M., Fan, J., Pan, W., Feng, Z., Su, Y., & Zhou, W. (2018). Structural characteristics and rheological properties of ovalbumin-gum arabic complex coacervates. *Food Chemistry, 260*, 1–6. https://doi.org/10.1016/j.foodchem.2018.03.141

Oettgen, H. C. (2023). Mast cells in food allergy: Inducing immediate reactions and shaping long-term immunity. *Journal of Allergy and Clinical Immunology, 151*(1), 21–25. https://doi.org/10.1016/j.jaci.2022.10.003

Olennikov, D. N., Kashchenko, N. I., Chirikova, N. K., Koryakina, L. P., & Vladimirov, L. N. (2015). Bitter gentian teas: Nutritional and phytochemical profiles, polysaccharide characterisation and bioactivity. *Molecules (Basel, Switzerland), 20*(11), 20014–20030. https://doi.org/10.3390/molecules201119674

Renz, H., Allen, K. J., Sicherer, S. H., Sampson, H. A., Lack, G., Beyer, K., & Oettgen, H. C. (2018). Food allergy. *Nature Reviews Disease Primers, 4*(1). https://doi.org/10.1038/nrdp.2017.98

Sathe, S. K., Liu, C., & Zaffran, V. D. (2016). Food Allergy. *Annual Review of Food Science and Technology, 7*, 191–220. https://doi.org/10.1146/annurev-food-041715-033308

Saarimäki, L., Kivistö, J., Palmu, S., Protudjer, J. L. P., Huhtala, H., & Karjalainen, J. (2023). Trends in severe allergic reactions of adults in Finland between 1999 and 2020: A national population study. *Allergy*. https://doi.org/10.1111/all.15929

Sahid, M. N. A., & Kiyoi, T. (2020). Mast cell activation markers for in vitro study. *Journal of Immunoassay & Immunochemistry, 41*(4), 778–816. https://doi.org/10.1080/15321819.2020.1769129

Simons, F. (2008). 9. Anaphylaxis. *Journal of Allergy and Clinical Immunology, 121*(2), S402–S407. https://doi.org/10.1016/j.jaci.2007.08.061

Tan, Y., Li, M., Kong, K., Xie, Y., Zeng, Z., Fang, Z., & Liu, Y. (2023). In vitro simulated digestion of and microbial characteristics in colonic fermentation of polysaccharides from four varieties of Tibetan tea. *Food Research International, 163*, Article 112255. https://doi.org/10.1016/j.foodres.2022.112255

Tao, H., Guo, L., Qin, Z., Yu, B., Wang, Y., Li, J., & Cui, B. (2022). Textural characteristics of mixed gels improved by structural recombination and the formation of hydrogen bonds between curdlan and carrageenan. *Food Hydrocolloids, 129*, Article 107678. https://doi.org/10.1016/j.foodhyd.2022.107678

Wahyu Wijaya, A. R. P. A. (2017). Functional colloids from proteins and polysaccharides for food applications. *Trends in Food Science & Technology, 68*, 56–69. https://doi.org/10.1016/j.tifs.2017.08.003

Wang, M., Chen, G., Chen, D., Ye, H., Sun, Y., Zeng, X., & Liu, Z. (2019). Purified fraction of polysaccharides from Fuzhuan brick tea modulates the composition and metabolism of gut microbiota in anaerobic fermentation in vitro. *International Journal of Biological Macromolecules, 140*, 858–870. https://doi.org/10.1016/j.ijbiomac.2019.08.187

Wang, S., Yang, J., Shao, G., Qu, D., Zhao, H., Yang, L., & Zhu, D. (2020). Soy protein isolated-soy hull polysaccharides stabilized O/W emulsion: Effect of polysaccharides concentration on the storage stability and interfacial rheological properties. *Food Hydrocolloids, 101*, Article 105490. https://doi.org/10.1016/j.foodhyd.2019.105490

Wang, Y., Li, Y., Liu, Y., Chen, X., & Wei, X. (2015). Extraction, characterization and antioxidant activities of Se-enriched tea polysaccharides. *International Journal of Biological Macromolecules, 77*, 76–84. https://doi.org/10.1016/j.ijbiomac.2015.02.052

Wang, Y., Shao, S., Xu, P., Chen, H., Lin-Shiau, S., Deng, Y., & Lin, J. (2012). Fermentation process enhanced production and bioactivities of oolong tea polysaccharides. *Food Research International, 46*(1), 158–166. https://doi.org/10.1016/j.foodres.2011.11.027

Weber, L., Wang, X., Ren, R., Wei, X., Zhao, G., Yang, J., & Wang, D. (2019). The development of a macromolecular analgesic for arthritic pain. *Molecular Pharmaceutics, 16*(3), 1234–1244. https://doi.org/10.1021/acs.molpharmaceut.8b01197

Xiang, G., Sun, H., Chen, Y., Guo, H., Liu, Y., Li, Y., & Wang, X. (2023). Antioxidant and hypoglycemic activity of tea polysaccharides with different degrees of fermentation. *International Journal of Biological Macromolecules, 228*, 224–233. https://doi.org/10.1016/j.ijbiomac.2022.12.114

Yuan, Q., Xie, Y., Wang, W., Yan, Y., Ye, H., Jabbar, S., & Zeng, X. (2015). Extraction optimization, characterization and antioxidant activity in vitro of polysaccharides from mulberry (*Morus alba* L.) leaves. *Carbohydrate Polymers, 128*, 52–62. https://doi.org/10.1016/j.carbpol.2015.04.028

Zhang, J., Liu, Q., Gu, F., Liu, Y., Zhou, Y., Li, Y., & Liu, G. (2023). Effects of Lactobacillus fermentation on Eucheuma spinosum polysaccharides: Characterization and mast cell membrane stabilizing activity. *Carbohydrate Polymers, 310*, Article 120742. https://doi.org/10.1016/j.carbpol.2023.120742

Zhang, Z., Sun, L., Chen, R., Li, Q., Lai, X., Wen, S., & Sun, S. (2024). Recent insights into the physicochemical properties, bioactivities and their relationship of tea polysaccharides. *Food Chemistry, 432*, Article 137223. https://doi.org/10.1016/j.foodchem.2023.137223

Zhang, Z., Zhao, Y., Han, Y., Yang, B., Lin, H., & Li, Z. (2022). The natural substances with anti-allergic properties in food allergy. *Trends in Food Science & Technology, 128*, 53–67. https://doi.org/10.1016/j.tifs.2022.07.004

Zhao, Z., Huangfu, L., Dong, L., & Liu, S. (2014). Functional groups and antioxidant activities of polysaccharides from five categories of tea. *Industrial Crops and Products, 58*, 31–35. https://doi.org/10.1016/j.indcrop.2014.04.004

Zheng, Z., Pan, X., Luo, L., Zhang, Q., Huang, X., Liu, Y., & Zhang, Y. (2022). Advances in oral absorption of polysaccharides: Mechanism, affecting factors, and improvement strategies. *Carbohydrate Polymers, 282*, Article 119110. https://doi.org/10.1016/j.carbpol.2022.119110